Published in final edited form as:
J Microsc. 2009 May ; 234(2): 124–129. doi:10.1111/j.1365-2818.2009.03153.x.

Assessment of Acridine Orange and SYTO 16 for in vivo imaging of the peritoneal tissues in mice

Joshua Anthony Udovich[1], **David G. Besselsen**[2], and **Arthur F. Gmitro**[1,3]

[1]Optical Sciences Center, University of Arizona, Tucson, AZ, USA, 85724

[2]University Animal Care, University of Arizona, Tucson, AZ, USA, 85724

[3]Department of Radiology, University of Arizona, Tucson, AZ, USA, 85724

Abstract

The effect of peritoneal injection of Acridine Orange (AO) and SYTO 16 in mice was investigated. Images of peritoneal tissues stained with these dyes and obtained through a confocal microendoscope are presented. Seventy-five Balb/c mice were split into five groups and given peritoneal injections of dye or saline. The proportions of negative outcomes in each group were compared using confidence intervals and the Fisher's exact statistical test. A statistically significant increase in adverse events due to dye injection was not observed.These data provide an initial investigation into the safety of AO and SYTO 16 for in vivo imaging.

Introduction

The confocal microendoscope (CME) is a new type of instrument for real-time in vivo imaging of tissue with cellular-level resolution. The two most common implementations of this technology are based on: 1) a confocal microscope coupled to a fiber optic imaging bundle(Gmitro and Aziz 1993; Lin and Webb 2000; Knittel, Schnieder et al. 2001; Sung, Richards-Kortum et al. 2003; Rouse, Kano et al. 2004; Yang, Raighne et al. 2005; Jean, Bourg-Heckly et al. 2007), which relays the image plane of the microscope to the tissue, or 2) a single fiber delivery system with the scanning mechanism of the confocal microscope built into the distal end of the imaging catheter(Dickensheets and Kino 1996; Polglase, McLaren et al. 2005; Shin, Pierce et al. 2007; Yelin, Boudoux et al. 2007). Although some systems are designed to work in reflectance, most are fluorescence-based imaging systems that utilize exogenous fluorescent dyes to achieve useful cellular contrast.

A number of fluorescent dyes including fluorescein, indocyanine green, and nuclear stains, such as acridine orange (AO), acriflavine (a molecule similar to AO), and SYTO dyes, have been used as contrast agents for confocal microendoscopic imaging. Investigators are exploring imaging applications in humans and/or animal models of colon cancer(de Wind, Dekker et al. 1998; Heijstek, Kranenburg et al. 2005), esophageal cancer(Opitz, Harada et al. 2002; Opitz, Quante et al. 2005; Kim, Nakagawa et al. 2006), lung cancer(Dutt and Wong 2006), and ovarian cancer(Roby, Taylor et al. 2000; Stakleff and Von Gruenigen 2003). In some of these applications, tissue micro-structure can be visualized using fluorescein, a dye approved by the FDA for retinal imaging. However, nuclear dyes are better at delineating the size, shape, and distribution of cell nuclei, which are important features for diagnosis in conventional histology. Promising results with the CME have been obtained during in vivo colon imaging in humans with acriflavine(Kiesslich, Burg et al.

*Corresponding author: gmitro@radiology.arizona.edu.

2004; Polglase, McLaren et al. 2005). We have shown that the CME can achieve high sensitivity and specificity for the detection of ovarian cancer using ex vivo human tissue stained with AO(Srivastava, Rodriguez et al. 2008). Due to the minimally invasive nature of the imaging technique, the CME also represents a powerful tool for studying disease development, progression, and regression in animal models. Imaging data can be collected from the same animal at multiple time points, reducing the number of animals required for research studies.

Although excellent image quality can be achieved with the CME using nuclear stains, there is concern about the cytotoxicity and potential mutagenicity of these materials. These dyes have been shown to cause damage to DNA(Epe, Pflaum et al. 1993) and to be mutagenic(Arshad, Farooq et al. 2006) to cells in culture. A clinical trial has indicated that AO used in conjunction with radiation therapy can help in the treatment of synovial sarcomas in humans(Kusuzaki, Murata et al. 2005). Clearly, dye safety is a concern for imaging in humans, but is also relevant when dyes are used in animals for repeated imaging sessions. This study was undertaken as a preliminary evaluation of the effects of AO and SYTO 16 on mouse tissues following peritoneal injection of the agents. Initial results were collected to determine if dye exposure caused elevated death rates compared to controls, and whether cytotoxic or mutagenic effects would be observed in internal organs due to dye exposure.

Materials and Methods

Ex Vivo Imaging

To show the general imaging properties of the dyes, selected tissue sites within the peritoneal cavity of euthanized mice were stained with AO or SYTO 16 (Invitrogen Corporation, Carlsbad, CA). The mice were sacrificed with an overdose of 2.5% Avertin and small incisions were made in their abdominal cavities to allow the imaging catheter of the CME to be inserted. Each imaging location received a localized exposure to 10 μL of either 0.33 mM AO or 20 μM SYTO 16. Animals used for visualization of dye-stained tissue were not a part of the statistical dye safety experiments.

Images were collected with a custom confocal microendoscope - an instrument designed to allow minimally invasive confocal imaging of tissues in humans or small animal models. Details of the system can be found in previous publications(Rouse, Kano et al. 2004; Rouse, Tanbakuchi et al. 2006; Makhlouf, Gmitro et al. 2008). Excitation light was provided by a diode-pumped solid-state laser (Coherent, Inc., Santa Clara, CA) operating at 488 nm. This laser light is shaped into a line through an anamorphic optical system and is scanned across a 30,000 element fiber-optic imaging bundle (Sumitomo Electric Industries, White Plains, NY). Emission light collected by the catheter is reflected back off the scan mirror and passed through a dichroic mirror, which separates the tissue fluorescence from reflected illumination. The fluorescent light is focused onto a confocal slit aperture that rejects a majority of the light collected from out-of-focus imaging planes. A second scan mirror relays the light through a 510 nm longpass filter and onto a Photometrics Cascade II CCD camera. With this optical system we are able to create full-frame two-dimensional confocal images at 30 frames per second. The in-plane resolution of the system is approximately 3 μm and the axial resolution is 25 μm.

Two different catheters were used for imaging. One catheter has a miniature objective lens located at the catheter tip to relay the end of the fiber bundle into the tissue with a magnification of 1.5 from tissue to fiber and an NA in tissue of 0.5. Imaging depth is controlled through movement of the fiber bundle relative to the lens, which is held in contact with the tissue surface. The diameter of this catheter is 3 mm and it is suitable for imaging

large organs. The second catheter is much smaller, at 1 mm in diameter, and consists of a bare fiber in contact with the tissue. The focal plane for this catheter is the end of the fiber, and the NA is approximately 0.35. The field of view of the bare fiber and miniature objective catheters is 720μm and 450μm, respectively.

Acridine orange and SYTO 16 both fluoresce when illuminated by 488 nm excitation light(Invitrogen Corporation, Carlsbad, California). AO has an emission maximum at 525 nm when bound to DNA. This maximum shifts to the red when AO is bound to RNA or concentrated in the cytosol or organelles such as lysosomes. SYTO 16 fluoresces at 518 nm when bound to DNA and 525 when bound to RNA. SYTO 16 binds preferentially to DNA over RNA at a ratio of approximately 20:1, and AO binds at a ratio of 3:1.

Animals and Treatment

Seventy five post-breeding BALB/c mice (~6 months, confirmed not pregnant) were purchased from Jackson Laboratories (Bar Harbor, ME) and split into five groups of fifteen: a control group, two groups injected with different concentrations of SYTO 16, and two groups injected with different concentrations of AO. All mice were mixed between cages (4 per cage) and housed within the University of Arizona Animal Care facility with free access to food and water. Animals were inspected daily and handled weekly by trained animal facility personnel.

Concentrations of dye used in this study represent 1X and 10X the standard in vivo imaging concentration. For the SYTO 16 groups, the concentrations of dye used were 20 μM and 200 μM. AO concentrations were 0.33 mM and 3.3 mM. Dyes were diluted in saline, and 250 μL of the dye mixture was injected into the peritoneal cavities of the mice. The control group received 250 μL injections of saline.

Tissue Acquisition and Histology

Mice from each group were euthanized at 1 month (6 animals), 3 months (20 animals) and 1 year (40 animals) after the initial dye injection with an overdose of 2.5% Avertin. In a few cases, an animal died prior to the 1, 3, or 12 month time point, and therefore one fewer animal was sacrificed in that cohort for that time point. Major organs collected from each animal included the liver, kidney, heart, lung, spleen, uterus, and mammary. Any abnormal growths were also collected from the animals, and all samples were fixed in formalin. Tissues were processed via standard histology methods, stained with hematoxylin-eosin, and mounted on slides.

Analysis

All tissue slides were inspected by a board-certified veterinary pathologist and individual animals were grouped into one of four categories based on pathology results: (1) all inspected tissues were considered normal for mice of this strain and age, (2) one or more of the tissues had a benign neoplasm, (3) one or more of the inspected tissues had a malignant neoplasm, and (4) the animal died prior to tissue harvesting. These four groups were then regrouped for statistical analysis. Normal and benign age-related neoplasms were considered as positive outcomes and malignant neoplasms and premature death were considered as negative outcomes. 95% confidence intervals were calculated for the proportion of negative outcomes for all of the groups using the adjusted Wald method(Sauro and Lewis 2005). The Fisher's exact test(Bland 1995) was used to test the null hypothesis that dye treatment does not cause an increase in negative outcomes between the control and test groups. One sided p-values for negative outcomes that were greater than the control group were calculated to test this hypothesis. Rejection of the null hypothesis for a single comparison of a dye treatment group and a control group would indicate that it is unsafe to use that particular dye

at that concentration for repeated in vivo imaging experiments. Ideally, the null hypothesis would be supported, suggesting that there is no statistical difference between the dye groups and the control group.

Results

Images of mouse tissue stained with AO and SYTO 16 are shown in figure 1. All images were collected with the confocal microendoscope using either the bare fiber catheter or the miniature objective catheter. Figures 1a-d were collected with AO as the contrast agent, and e-h with SYTO 16. Figures 1a and 1e show the inside of the peritoneal cavity wall imaged with a bare fiber on the confocal microendoscope. Figures 1b and 1f show the same tissue using the catheter with the miniature objective. Striations of the muscle and the nuclei of cells are clearly visible in these images. Figures 1c and 1g show images of mouse ovary obtained with the bare fiber catheter, with the brightest spots being nuclear regions and surrounding areas showing some fluorescence from the cytoplasm. Figures 1d and 1h are images of a tumor mass inside of a mouse, also obtained with the bare fiber.

Of the 75 mice that began the study, 66 survived to have tissues harvested, with the premature deaths distributed fairly evenly among the five groups (Table 1). Animals that died prior to being euthanized were unable to have tissue examined histologically, and were placed in a separate early death category.

There were multiple types of benign conditions identified, all of which occur with relatively high frequency in aged BALB/c mice. The most common non-neoplastic change was the development of bronchoalveolar adenoma (one animal from low SYTO 16, two animals from high SYTO 16, one animal from the control group, and two animals from low AO concentrations). Other benign lesions included duodenal adenoma (two animals from high AO and one animal from high SYTO 16 concentrations), keratoacanthoma (one high SYTO 16), trichoepithelioma (high AO), and mammary myoepithelioma (one low SYTO 16). These are not uncommon to find in animals of the BALB/c strain at an advanced age.

Four types of malignant tumors were found in the mice. Mammary adenocarcinoma (one animal each from the control and low SYTO 16 groups), and follicular center-cell type lymphoma (one animal each from control and high SYTO 16 groups, two from low AO group, and three from high AO group) were identified. Other malignant tumors were histiocytic sarcoma (one low AO in the spleen and one control animal in the mesenteric lymph node) and bronchoalveolar adenocarcinoma (one animal from the high SYTO 16 group, and the same animal that developed lymphoma). These malignant tumors are also commonly observed in BALB/c mice at this age.

Due to the low frequency of occurrence for a few of the outcomes, as shown in Table 1, the four outcomes were grouped into two for statistical analysis. Animals with normal or benign neoplasms were grouped together as “positive” outcomes while malignant neoplasm and death prior to the conclusion of study were grouped together as “negative” outcomes.

Grouping in this manner allowed proportions of negative outcomes to be evaluated using the adjusted Wald interval for 95% percent inclusion within the interval. This method provides a conservative estimate for comparing the negative outcomes of all groups relative to one another. If two confidence intervals do not overlap, there is at least 95% certainty that the two groups are significantly different. Table 2 provides the results of a confidence interval calculation, and a graphical representation of this is given in figure 2.

Each of the test groups was also compared to the control group using a one-sided Fisher's exact test to determine if the null hypothesis could be rejected. A one-sided test was used

because the test is evaluating the negative effect due to dye treatment. P-values less than 0.05 indicate that we can reject the null hypothesis of no difference with 95% confidence for the given dye and concentration. The results of this test are shown in Table 3.

Discussion

Acridine Orange and SYTO 16 are both effective at staining the DNA of cells and showing specific information about cell nuclei, such as size and distribution. Figure 1 shows tissues stained with AO or SYTO 16. SYTO 16 preferentially binds to DNA over RNA at a ratio of 20:1, whereas for AO the ratio is 3:1. This results in slightly different looking images for the two dyes in similar regions of mouse tissue. Typically normal tissues have a homogeneous nuclear and tissue structure, whereas cancerous tissues will be more heterogeneous. Although the images shown were obtained in euthanized mice for experimental convenience, the results show that the imaging configuration is well suited for use in imaging live mice for investigating tumor growth models.

Results of the confidence intervals and the Fisher's exact test indicate that there is not a statistically significant difference between the control and test groups. Figure 2 shows that all of the confidence intervals overlap. We are unable to reject the null hypothesis using this method, as these results show graphically that there is a large overlap between the expected proportions of negative outcomes in both control and dye treated animals. Table 3 presents results from the Fisher's exact test. All of the p-values are greater than 0.05, meaning that for the conditions of this study, we cannot reject the null hypothesis.

The general observations on these animals, the confidence intervals on the proportions of negative outcome, and the statistical analysis indicate that, for the conditions of this study, there is not a significant observable effect on the animals due to dye treatment. A majority of the animals included in the study had no abnormal pathology findings. These observations suggest that there is not a readily observed malignant or morbid effect due to the treatment. Tissues from treated animals investigated by pathology did not stray from observations of the control group or from expected conditions in animals of this strain or age. Indeed, the lesions observed in the groups are common in aged BALB/c mice. Similar mortality rates were observed among the treatment and control groups. Results from the confidence intervals show that there is significant overlap of the expected proportion of negative outcomes for the test and control groups. Similarly, the results of the Fisher's exact test clearly do not allow rejection of the null hypothesis because all of the p values calculated are greater than 0.05.

Due to the small sample sizes (resulting in low statistical power), our confidence in not rejecting the null hypothesis is low. This means that there is a high probability of a type II error (failure to reject the null hypothesis when it should be rejected). Although this study cannot be used to verify the null hypothesis that there is no effect due to the injection of dye, it does indicate that the effect, if any, is small (i.e. large proportions of the animals did not die or develop malignant neoplasms with peritoneal injection of the dye compounds). In fact, the groups of animals treated with SYTO 16 had a lower proportion of negative outcomes than the control group, which on face value indicates a potentially positive effect due to treatment with the dye. This is almost certainly not the case and is most likely a result of the small sample size. Studies with larger sample sizes will have to be done to assess the more subtle effects of the dye treatment. This work provides a foundation for further studies with larger animal populations that will allow researchers to more accurately determine the effects of dye use on animals when injected peritoneally for repeated in vivo imaging experiments within the abdominal cavity.

Conclusion

Acridine orange and SYTO 16 are able to stain specific components of cells. When used in conjunction with the confocal microendoscope, these contrast agents provide useful cellular-level images of tissue. The dyes are well suited for imaging applications inside the peritoneal cavities of live anesthetized mice.

The null hypothesis, that there is no difference between a control group and treatment groups receiving dye injections, was unable to be rejected in this study. Confidence intervals, calculated using the adjusted Wald method, overlapped for all of the test and control groups. Results of the one-sided Fisher's exact test also support that we are unable to reject the null hypothesis, as all p-values were greater than 0.05. Peritoneal tissues of mice from the test groups, inspected by a board-certified veterinary pathologist, showed similar lesions to those seen in the control group. Ideally this study would verify the null hypothesis; this was not possible due to limited population size. However, for the conditions of this study, there is not a significant observable effect on the animals due to dye treatment. Further studies must be conducted to more accurately determine the effect of these dyes on the peritoneal tissues of mice.

Acknowledgments

The authors wish to thank Christine Howison at the Arizona Health Science Center for help in preparing animals. This work was supported by a Grant from the Arizona Disease Control Research Commission number 971 and NIH grants 1 R21 CA 113964-01A1 and 5 R01 CA 1158780.

References

Arshad R, Farooq S, et al. Mutagenic effect of acridine orange on the expression of penicillin G acylase and -lactamase in Escherichia coli. Letters in Applied Microbiology. 2006; 42:94–101. [PubMed: 16441371]

Bland, M. An Introduction to Medical Statistics. Oxford University Press; Oxford: 1995.

de Wind N, Dekker M, et al. Mouse Models for Hereditary Nonpolyposis Colorectal Cancer. Cancer Res. 1998; 58(2):248–255. [PubMed: 9443401]

Dickensheets DL, Kino GS. Micromachined scanning confocal optical microscope. Opt. Lett. 1996; 21(10):764. [PubMed: 19876151]

Dutt A, Wong K-K. Mouse Models of Lung Cancer. Clin Cancer Res. 2006; 12(14):4396s–4402. [PubMed: 16857817]

Epe B, Pflaum M, et al. DNA damage induced by photosensitizers in cellular and cell-free systems. Mutation Research. 1993; 299(3-4):135–145. [PubMed: 7683082]

Gmitro AF, Aziz D. Confocal microscopy through a fiber-optic imaging bundle. Opt. Lett. 1993; 18(8):565. [PubMed: 19802201]

Heijstek MW, Kranenburg O, et al. Mouse Models of Colorectal Cancer and Liver Metastases. Digestive Surgery. 2005; 22(1-2):16–25. [PubMed: 15838167]

Jean F, Bourg-Heckly G, et al. Fibered confocal spectroscopy and multicolor imaging system for in vivo fluorescence analysis. Opt. Express. 2007; 15(7):4008–4017. [PubMed: 19532645]

Kiesslich R, Burg J, et al. Confocal laser endoscopy for diagnosing intraepithelial neoplasias and colorectal cancer in vivo. Gastroenterology. 2004; 127(3):706–713. [PubMed: 15362025]

Kim S-H, Nakagawa H, et al. Tumorigenic Conversion of Primary Human Esophageal Epithelial Cells Using Oncogene Combinations in the Absence of Exogenous Ras. Cancer Res. 2006; 66(21): 10415–10424. [PubMed: 17079462]

Knittel J, Schnieder L, et al. Endoscope-compatible confocal microscope using a gradient index-lens system. Optics Communications. 2001; 188(5-6):267–273.

Kusuzaki K, Murata H, et al. Clinical Outcome of a Novel Photodynamic Therapy Technique Using Acridine Orange for Synovial Sarcomas&para. Photochemistry and Photobiology. 2005; 81(3): 705–710. [PubMed: 15686440]

Lin CP, Webb RH. Fiber-coupled multiplexed confocal microscope. Opt. Lett. 2000; 25(13):954–956. [PubMed: 18064238]

Makhlouf H, Gmitro AF, et al. Multispectral confocal microendoscope for in vivo and in situ imaging. Journal of Biomedical Optics. 2008; 13(4):044016–9. [PubMed: 19021344]

Opitz OG, Harada H, et al. A mouse model of human oral-esophageal cancer. J Clin Invest. 2002; 110(6):761–769. [PubMed: 12235107]

Opitz OG, Quante M, et al. A Mouse Model of Oral-Esophageal Carcinogenesis. Onkologie. 2005; 28(1):44–48. [PubMed: 15696643]

Polglase AL, McLaren WJ, et al. A fluorescence confocal endomicroscope for in vivo microscopy of the upper- and the lower-GI tract. Gastrointestinal Endoscopy. 2005; 62(5):686–695. [PubMed: 16246680]

Roby KF, Taylor CC, et al. Development of a syngeneic mouse model for events related to ovarian cancer. Carcinogenesis. 2000; 21:585–591. [PubMed: 10753190]

Rouse AR, Kano A, et al. Design and Demonstration of a Miniature Catheter for a Confocal Microendoscope. Appl. Opt. 2004; 43(31):5763–5771. [PubMed: 15540433]

Rouse AR, Tanbakuchi AA, et al. Design of an in-vivo multi-spectral confocal microendoscope for clinical trials. Proc. SPIE Int. Soc. Opt. Eng. 2006; 6082

Sauro, J.; Lewis, J. Estimating completion rates from small samples using binomial confidence intervals: comparisons and recommendations. Proceedings of the Human Factors and Ergonomics Society 49th Annual Meeting; 2005. p. 2100-2104.

Shin H-J, Pierce MC, et al. Fiber-optic confocal microscope using a MEMS scanner and miniature objective lens. Opt. Express. 2007; 15(15):9113–9122. [PubMed: 19547251]

Srivastava S, Rodriguez JJ, et al. Computer-aided identification of ovarian cancer in confocal microendoscope images. Journal of Biomedical Optics. 2008; 13(2):024021–13. [PubMed: 18465984]

Stakleff KDS, Von Gruenigen VE. Rodent models for ovarian cancer research. International Journal of Gynecological Cancer. 2003; 13:405–412. [PubMed: 12911715]

Sung K-B, Richards-Kortum R, et al. Fiber optic confocal reflectance microscopy: a new real-time technique to view nuclear morphology in cervical squamous epithelium in vivo. Opt. Express. 2003; 11(24):3171–3181. [PubMed: 19471442]

Yang L, Raighne AM, et al. Confocal microscopy using variable-focal-length microlenses and an optical fiber bundle. Appl. Opt. 2005; 44(28):5928–5936. [PubMed: 16231800]

Yelin D, Boudoux C, et al. Large area confocal microscopy. Opt. Lett. 2007; 32(9):1102–1104. [PubMed: 17410249]

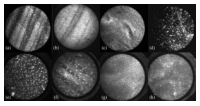

Figure 1.

Images of mouse tissue obtained with the confocal microendoscope. AO was used as a contrast agent in the top row of images, and SYTO 16 was used on tissues shown in the lower images. (a, b, e, and f) are of the peritoneal wall, (c,g) are images of the surface of the ovaries, and (d,h) show images of a tumor. All images shown were obtained with bare fiber catheter, except b and f, which used a catheter with a miniature objective to achieve higher magnification.

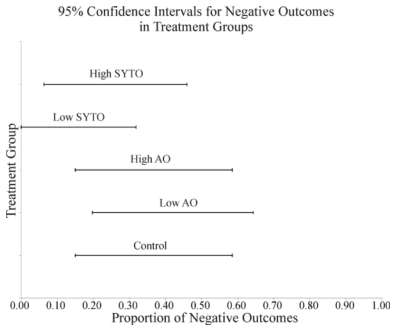

Figure 2.
Graphical representation of data presented in Table 3 showing confidence intervals for the proportion of negative outcomes for each of the treatments.

Table 1

Groups of outcomes for various treatments of BALB/c mice. A total of 75 animals were included in the test and all analysis of tissue was performed by a boardcertified veterinary pathologist.

	Normal	Benign Neoplasm	Malignant Neoplasm	Death Prior to Conclusion of Study	Total
Saline Control Group	9	1	3	2	15
Low AO concentration	6	3	3	3	15
High AO concentration	8	2	3	2	15
Low SYTO 16 concentration	12	2	1	0	15
High SYTO 16 concentration	8	4	1	2	15

Table 2

Lower and upper limits for the proportion of negative (malignancy or animal death prior to the conclusion of study) outcomes given the observed proportion in the study. These values were calculated using the exact binomial confidence interval and represent a 95% confidence.

Treatment	Negative Proportion	Lower Limit	Upper Limit
Control	0.333	0.150	0.585
Low AO	0.400	0.198	0.643
High AO	0.333	0.150	0.585
Low SYTO	0.067	<.0001	0.318
High SYTO	0.2	0.063	0.460

Table 3

One-sided P values for the Fisher's exact test.

Treatment	One-sided P value
Low AO	0.500
High AO	0.650
Low SYTO	0.991
High SYTO	0.893